Interaction of Dynamic Magnetic Fields with Magnetic Particles Immobilized at Lysosomes

M. Koch, J. Wiest

***Abstract*—In this study superparamagnetic iron oxide particles (Spions) were employed. The Spions were loaded with antibodies for the lysosomal membrane and moved by a dynamic magnet field above an adherent cell layer. A virus trying to invade a cell is emulated by the particle's rolling motion above the cell's surface. An invasion of the beads into the cells was finally accomplished endocytotically (First step). Then, inside the cells, close to the lysosomal membrane, the Spions were immobilized due to a covalent antigen/antibody binding. A following wiggle action (Second step) could permeabilize the lysosomal membrane, setting free aggressive enzymes inside the cytosol, which provoked apoptosis.**

***Index Terms*—Apoptosis, Dynamic magnetic field, Lysosomes**

I. Introduction

A) Introduction to the Maxwell equations

J. C. Maxwell (Fig.1) wrote in 1855 his famous set of equations in order to establish a mathematical description of Faraday's ideas about electro-magnetism [1]).

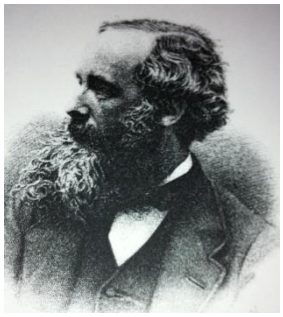

Fig. 1. James Clerk Maxwell (1831-1879), (Source: Wikipedia).

Regarding these equations Heinrich Hertz said "… they have their own existence and intelligence and they are smarter than we are. We can get more out of them than originally was placed into them …" [2]. In Fig. 2 our preferred order of the equations is shown, stating the most important Maxwell equation printed as the first one (with H: Magnetic field, J: Current density, D: Electric flux density, t: Time, E: Electric field, B: Magnetic flux density, ρ : Charge density).

Fig. 2. The Maxwell equations printed in the Danish newspaper Politiken on Apr, 1st 1992.

$$\nabla \times \vec{H} = \vec{J} + \frac{\partial \vec{D}}{\partial t} \tag{1}$$

$$\nabla \times \vec{E} = -\frac{\partial \vec{B}}{\partial t} \tag{2}$$

$$\nabla \cdot \vec{B} = 0 \tag{3}$$

$$\nabla \cdot \vec{D} = \rho \tag{4}$$

Maxwell's equations are the basis for the description of all electric events [3]. The first of them (1) connects magnetic with electric values. Though the current density equals always zero in between the plates of the capacitor (Fig.3), it is possible to have a current flowing in the connecting wires, e.g. an AC current.

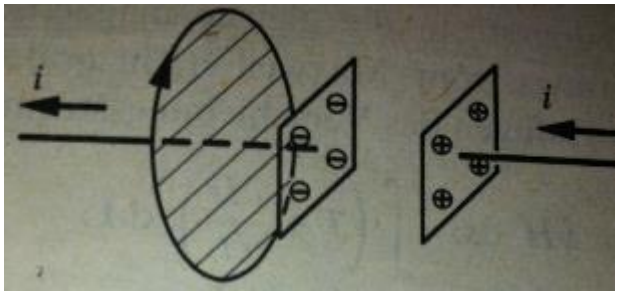

Fig. 3. The current i, which is flowing across the striped area $\vec{A}$ generates a magnetic $\vec{H}$-field along the border line of $\vec{A}$.

This work was supported in part by the Pavlick Research Society – Hosena / Germany.

M. Koch is with Stetter Elektronik, 64342 Seeheim-Jugenheim, Germany (e-mail: mko@mail.tele.dk).

J. Wiest is with cellasys GmbH – R&D, 80802 Munich, Germany (e-mail: wiest@cellasys.com).

Though no galvanic current is passing the integration area in Fig. 4, Maxwell has introduced - in order to make (1) mathematically correct - a so called "Displacement current" $\frac{\partial \vec{D}}{\partial t}$. This displacement current density is more or less an alternating electric field. Herewith Maxwell predicted already in 1856 the prospective existence of oscillators. These devices were invented by Heinrich Hertz roughly 50 years later.

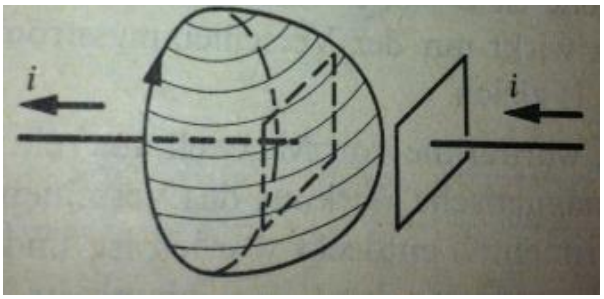

Fig. 4. No galvanic current passes the striped and bended integration area, but a force field may exist due to i. In order to fulfill (1), Maxwell introduced the displacement current.

B) Magnetic versus Electro-magnetic

If the Maxwell equations are able to describe all electric events, they should also be able to explain the difference between electro-magnetism and magnetism.
Equation (1) connects magnetic (H) and electric (J,D) values.

$$\vec{D} = \varepsilon \hat{\vec{E}} \sin \omega t \tag{5}$$

$$\frac{\partial \vec{D}}{\partial t} = \omega \varepsilon \hat{\vec{E}} \cos \omega t \tag{6}$$

With (5) respectively (6) and with setting up boundary conditions as $f = 10Hz$, $\varepsilon_r = 10$, $\hat{\vec{E}} = 10^6 V/m$ and $\omega t = 0$ it is possible to calculate $\frac{\partial \vec{D}}{\partial t} = 5 \cdot 10^{-9} \frac{A}{mm^2}$ (with ε: Permittivity, ω: Angular velocity, *f*: Frequency). The maximal available current density in a copper wire of approximately $J = 2.5 \frac{A}{mm^2}$ suggests to produce a low frequent magnetic force field $\vec{H}$ due to a galvanic current $\vec{J}$ and not by means of a displacement current $\frac{\partial \vec{D}}{\partial t}$. Having a factor of approximately 1.000.000.000 between current density and displacement current, the first Maxwell equation (equ.1) is reduced for practical applications in this very low frequency range to:

$$\nabla \times \vec{H} = \vec{J} \tag{7}$$

This is a very important aspect for application in physiological solutions (water including ions): By having a purely "magnetic" field and by evading the electrical material constants $\varepsilon_0 \varepsilon_r$, heating effects can be avoided. In contrary with high frequencies, alternating in the range of MHz, GHz or even THz the original equation (1) is valid in order to describe the field completely. Herewith the electric material constants show up again (and the heating effects) and the field comes to be "electromagnetic".

C) Experimental Example

An experiment indicating a magnetic force, which is holding a washer made from soft iron (magnetite disc) below a magnetic field return stack is described (see [4] for video). In figure 5 the various steps from "rest position" via "jumping of the magnetite disc" and "hovering of the magnetite disc" to "rotation of the magnetite disc" are pictured.

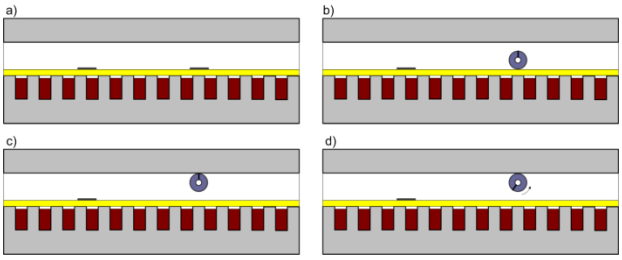

Fig. 5. Effects on the copper disc (left) and the magnetite disc (right) due to the application of a magnetic field. a) Rest position; b) Only the magnetite disc moves and jumps around in random manner; c) The random behavior stops and the magnetite disc hovers below a return path of the magnetic field; d) The magnetite disc rotates, which indicates hysteresis effects [3].

A magnetic holding force arresting the magnetite disc, must be

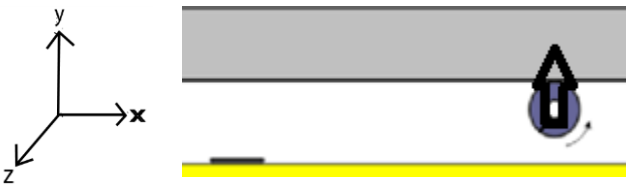

Fig. 6. This image shows, that the magnetic field $\vec{B}$, established by the field generator (yellow area), is concentrated on top of the washer. This top area is saturized (arrow) meaning, that all the field lines are in parallel and all the spins $\vec{m}$ in the washer are in line with this field.

– a priori - derived out of the gradient-force. See equations (8) to (13) and figure 6.

In the important top area of the washer (The main area of interest here), where the device is touching the field return path, a force with a magnetic character $\vec{F}_g$ is formed. $\vec{F}_g$ is strong enough to urge the washer with a pressure of σ_y in y direction against the field return path.

$$\vec{F}_g = (m\nabla)\cdot\vec{B} \tag{8}$$

$$\begin{aligned}\vec{F}_g &= m_x\cdot\frac{\partial}{\partial x}\cdot(\vec{e}_x\cdot\vec{e}_x)\cdot B_x\cdot\vec{e}_x + \\ &m_y\cdot\frac{\partial}{\partial y}\cdot(\vec{e}_y\cdot\vec{e}_y)\cdot B_y\cdot\vec{e}_y + \\ &m_z\cdot\frac{\partial}{\partial z}\cdot(\vec{e}_z\cdot\vec{e}_z)\cdot B_z\cdot\vec{e}_z\end{aligned} \tag{9}$$

$$\vec{F}_g = m_x\cdot\frac{\partial B_x}{\partial x}\cdot\vec{e}_x + m_y\cdot\frac{\partial B_y}{\partial y}\cdot\vec{e}_y + m_z\cdot\frac{\partial B_z}{\partial z}\cdot\vec{e}_z \tag{10}$$

$$\vec{F}_g = m_y\cdot\frac{\partial B_y}{\partial y}\cdot\vec{e}_y \tag{11}$$

The pressure $\frac{\vec{F}_g}{\partial z\cdot\partial x}$ is defined, in equation (12).

$$\frac{\vec{F}_g}{\partial z\cdot\partial x} = \mu_0\cdot m_y\cdot\frac{\partial H_y}{\partial x\partial y\partial z}\cdot\vec{e}_y \tag{12}$$

In equation (13) the focus is on one magnetic pole, in other words: On one end of a dipole.

$$\begin{aligned}\frac{\vec{F}_g}{\partial A} &= (+)\sigma_y\cdot\vec{e}_y = \mu_0\cdot(\pm)m_y\cdot\frac{(\pm)\partial H_y}{\partial x\partial y\partial z}\cdot\vec{e}_y = \\ &\mu_0\cdot(\pm)m_y\cdot\vec{e}_y\cdot\frac{(\pm)(\nabla\cdot H)}{\partial A}\end{aligned} \tag{13}$$

The following boundary conditions are used for the calculation:

$$\mu_0 = 4\cdot\pi\cdot10^{-7}\left[\frac{Vs}{Am}\right];\ \frac{\partial H_y}{\partial x\partial y\partial z} = \frac{5\cdot10^5\,A/m}{1(nm)^3};\ 8Fe^{2+};$$

$$\frac{4\ unpaired\ \ electrons}{Fe^{2+}};\ BohrMagneton\ \ \mu_B = 9.27\cdot10^{-24}\left[Am^2\right]$$

The values for one elementary cell [6] are:

$$\sigma = \frac{4\cdot\pi\cdot10^{-7}\left[\frac{Vs}{Am}\right]\cdot8\cdot4\cdot9.27\cdot10^{-24}\left[Am^2\right]\cdot5\cdot10^5\left[A/m\right]}{10^{-27}\left[m^3\right]} =;$$

$$1.85\cdot10^5\,\frac{N}{m^2}$$

$$1kp = 9.81N;\ \sigma = \frac{0.185[kp]}{9.81\left[mm^2\right]} = 18.8\left[\frac{p}{mm^2}\right]$$

The conclusion of the experiment is that the magnetite disc (weight 2.3 g) is forced against the field return way with a pressure of $19\left[\frac{p}{mm^2}\right]$.

II. Materials and Methods

A) Material, Procedures and Particles

The magnetite disc used in the previous experiment was made out of soft iron, and macroscopically structured in "Weiss domains"[5] with movable "Bloch walls"[6]. Only one elementary cell of the crystalline disc structure (contact point washer/field-return-way) - like postulated in the numerical evaluation of the above experiment, with 8 active Fe^{2+} ions - would be enough to hold the washer in a hovering position beneath the field return way. The washer experiment was also conducted in order to take notice of rotational micro effects in a macroscopic way. The dynamic force field $\vec{H}$ jammed into the crystalline structures of the washer is provoking macroscopic reaction. Said more specific: The spins of the unpaired spion-electrons are synchronized with the dynamic magnetic field from the outside and the field energy is converted into a kinetic turning motion of the magnetite disc.

The field-powered rotating magnetite disc gave birth to the idea of applying dynamic fields onto biological- and material-nanostructures. The area of nanomaterial applications is large and their solicitation in cell biology is enormous and it might be possible to influence the cell fate non-invasively via field-particle interaction.

At first it is important to be non-invasive, which makes the research more correlated to the in vivo cell biology. Secondly, predictable therapeutic applications are desirable. The third aspect is to generate a reliable computer model of field - and particle-interaction, which demands a relatively simple

crystalline structure of the particle while the field structures are defined by the device.

In 2002 Prof. Braeuchle from LMU/Munich observed a virus – dyed with fluorescence molecules - entering a living cell [7-10]. The virus moved above the cell surface, until the correct receptor was met, which initiated an endocytotical virus transfer into the interior of the cell. Our idea was to transfer magnetic particles likewise into living human cells. The optimal size of the particles ((20nm – 100nm) and their structure (superparamagnetic) was investigated. The kind of field, which should be applied (slowly moving (dynamic magnetic, avoiding heat development)), was determined.

B) Magnetized structures

Very small iron oxide particles (low nano-meter width), contain only elementary cells (no "Bloch walls") and they show no residual magnetism after the external field vanishes. These particles are called "Spions" (superparamagnetic-ironoxide-nanoparticles).

The field device generates a dynamic force field, which is converted inside the particle into a magnetic flux field B, which operates on a "Spion" particle with a magnetic moment $\vec{M}$ and a moment of inertia I. The field generates a torque $\vec{\tau}$ equal to $\vec{\tau} = \vec{\mu} \times \vec{B}$ (Fig.7).

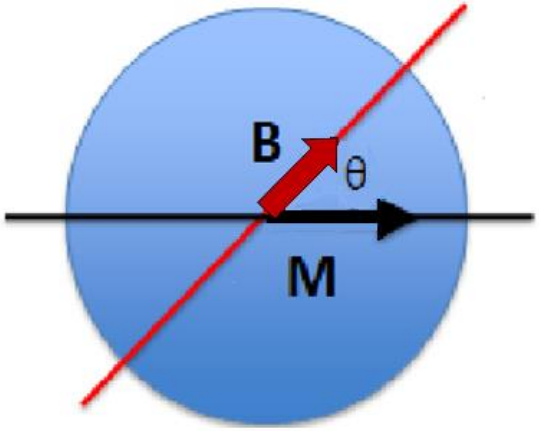

Fig. 7. Device produced flux density B, which is seen by the "Spion" particle as a circulating field event. This circulating vector field provides a changing torque on the particle proportional to (m, B).

The magnetic spin vectors of a Spion are spinning in the GHz range at room temperature. However, the spins can be synchronized with the incoming dynamic magnetic field of marginal field strength. Herewith our incoming magnetic field, produced by a dynamic field generator (Fig.8), enables to roll the nano-particles above the cell surface until a proper receptor is met.

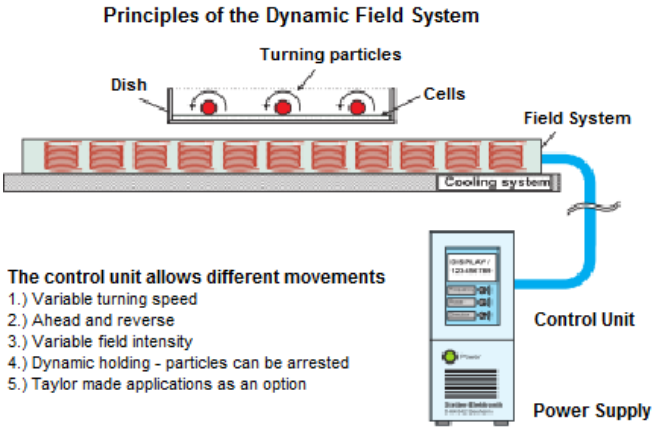

Fig. 8. The field generator produces a dynamic field, which moves every single magnetic particle above the cells.

As detailed in Fig. 9 the above field device moves and turns every single "Spion" individually.

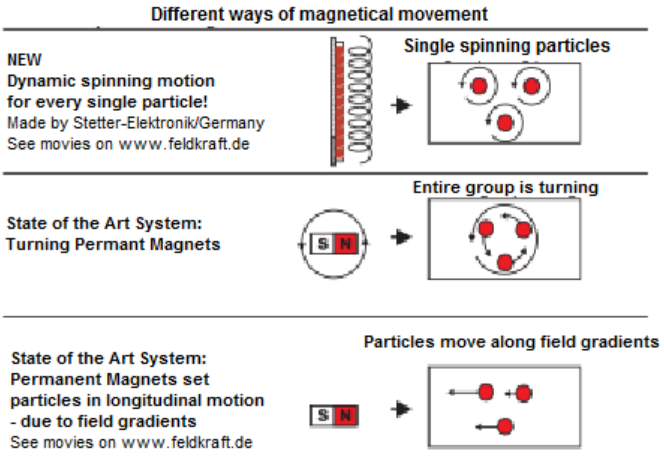

Fig.9. A taylormade field device produces a spinning motion for every single particle.

C) Cell invasion and immobilization inside the lysosomes

If the rolling particle is hitting a proper receptor [7-10], it is endocytoticly transferred into the cell interior ending inside the lysosomes in order to be digested. However, before the rolling on the surface was started, antibodies were covalently attached to the particle, which are able to bind to transmembrane proteins on the inside of the cell organelle. The Spion particles became immobilized in such a way, that they were not able to roll any longer, but they can wiggle the lysosome membrane, hereby permeabilizing it as pictured in figure 10 and figure 11.

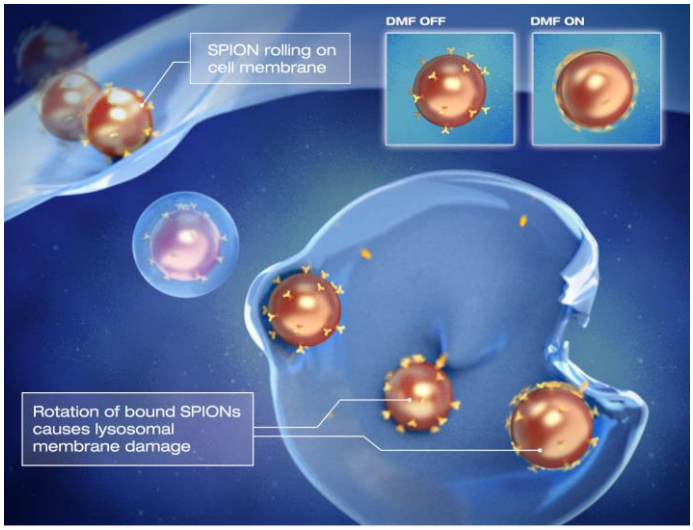

Fig.10. Artistic impression of how the Dynamic Magnetic Field (DMF) initiates particle internalization into the lysosome (Source: [15]).

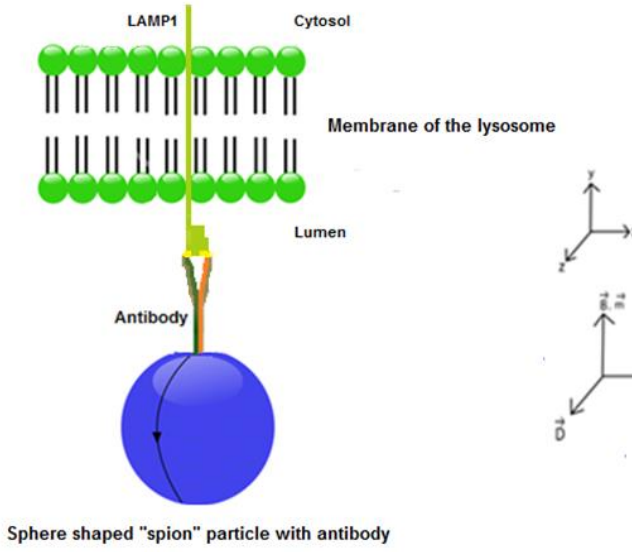

Fig.11: A y-formed antibody (to LAMP1), which is connected to the dextran layer on the "Spion-sphere", binds on an antigen. The antigen is integrated in the membrane of the lysosome. The spins of the "Spions" directed before into the x-axis, align their magnetic moment $\vec{M}$ with the incoming (y-axis) device generated dynamic magnetic field density $\vec{B}$. Hereby a torque $\vec{\tau}$ is created, which is turning the "Spion-sphere" (bended arrow line).

IV. Results

Lysosomes are acidic organelles in eukaryotic cells. Their main task is to digest macromolecules and they may be regarded as the "cell's stomach".

The lysosomal membrane must prevent accidental release of the acidic lysosomal lumen or lysosomal enzymes into the cytosol. Therefore the lysosomal membrane contains highly glycosylated proteins, whose complex intraluminal carbohydrate side chains form a coat on the inner surface of the membrane [11]. These glycoproteins may serve as a barrier towards the cytosol. Changes inside the membrane structure can result in a lysosomal destabilization. It has been proposed [12-14] that lysosomal proteases, in particular cathepsin B, can amplify their own liberation. Small amounts of released cathepsin B trigger the lysosomal membrane to permeabilize and herewith apoptosis of the cell. Fig.12a,b,c, are documenting these events [15].

Fig.12a "End of the first phase: INVASION": The antibody carrying particles (Fluorescents-Dye: Red) had come into the cells. Cell-lysosomes (dyed with Lysotracker-Green) are containing the particles (red), which can be seen in a colocation (yellow) on the right side of the first picture. Fig.12b "End of the second phase: Permeabilization of Lysosome-Membrane": After the invasion a dynamic magnetic force field generated from the device outside of the dish, grips the immobilized particles and generates magnetic torques, which destabilizes the lysosomal membrane facilitating lysosomal enzymes to be spread out into the cytosol. Consequently the green dyes vanish and in parallel the colocation color yellow.

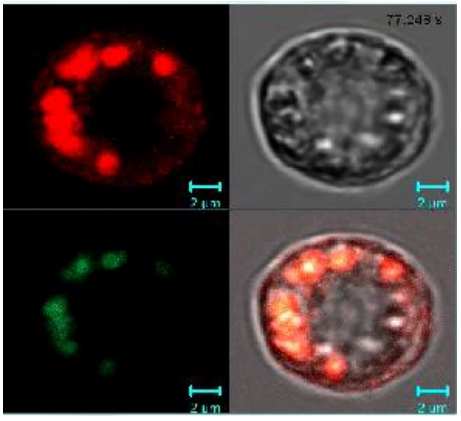

Fig.12a "End of the first phase: INVASION"

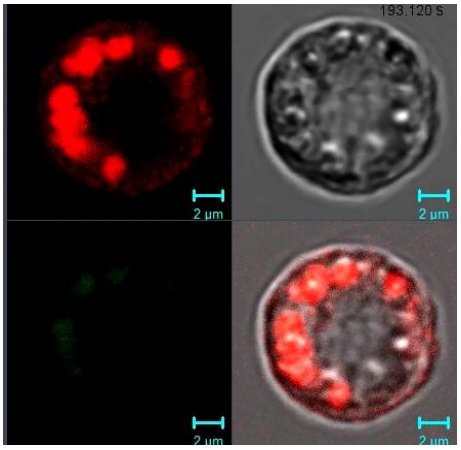

Fig.12b "End of the second phase: Permeabilization of Lysosome-Membrane"

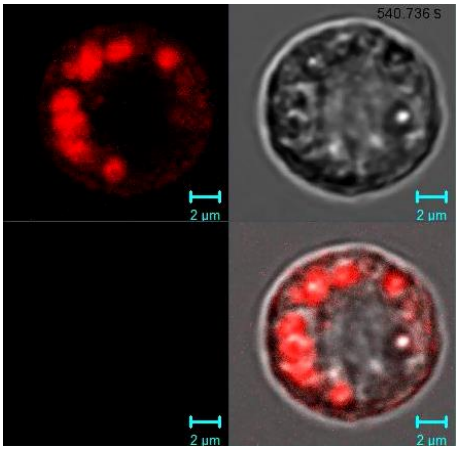

Fig.12c "Third phase: Apoptosis"

Fig.12c "Third phase: Apoptosis": The cells are dying a regulated cell death. On the last slide no tracker-dye and no yellow colocation are visible.
Cancer cells inside a tumor might be able to eliminate (pumping out of the cytosol) roving enzymes fast enough, so that these cells avert apoptosis. However the former lysosome (pH 5) enzymes might attack neighbor cells inside the tumor tissue (pH 5), when reactivated inside the acidic surrounding [15].

V. Discussion

We state that low frequent force fields have magnetic character. They do not possess material constants, which avoids heating. Their magnetic forces/torques make "Spion" particles roll above the cell surface. Hereby the particles, bearing covalently attached antibodies, reach the lysosomes and permeabilize them, due to magnetic wiggling of the lysosome membrane. Magnetically provoked lysosomal membrane penetration starts a regulated cell death procedure, without any heat generation.

VI. References

10. References

[1] J.C.Maxwell, "On Faraday Lines of Force" The Scientific Papers of James Clerk Maxwell, Cambridge University Press, 1890, Vol.1, P. 153.
[2] Quoted after Morris Kline: Mathematics and the search for knowledge, Oxford University Press, New York, 1985, P. 144.
[3] G.Bosse, „Grundlagen der Elektrotechnik" , BI Mannheim, 1967.
[4] http://www.feldkraft.de/Filme/Spring.wmv.
[5] W. D.Callister,Jr., "Fundamentals of Materials Science and Engineering", John Wiley and sons, Inc., 2001.
[6] F.Bloch, „Zur Theorie des Austauschproblems und der Remanenzerscheinung der Ferromagnetika", Zeits.f.Physik 74, 1932.
[7] G. Seisenberger, M. U. Ried, T. Endress, H. Buenung, M. Hallek, Ch. Braeuchle, " Real Time Single Molecule Imaging of the Infection Pathway of an Adeno –assossiated Virus", Science 30, Vol.294 no. 5548 pp. 1929-1932, 2001.
[8] F.M. Mickler, L. Moeckel, N. Ruthardt, M. Orgis, E. Wagner, C. Braeuchle, "Tuning nanoparticle uptake: Live-cell imagin reveals two distinct endocytosis mechanisms mediated by natural and artificial EGFR targeting ligand", Nano Lett. 12(7),p. 3417 , 2012.
[9] C. Braeuchle, G. Seisenberger, T. Endress, M.U. Ried, H. Buening M. Hallek, "Single Virus Tracing: Visualisation of the Infection Pathway of a virus into a Living Cell", ChemPhysChem, p.299, 2002.
[10] M.Goebel, T. Endress, C.Braeuchle, „Visualisierung einzelner Viren auf ihrem Infektionsweg in lebende Zellen", Laborwelt IV, 2002.
[11] A.C. Johansson, H.Appelqvist, C.Nilsson, K.Kågedal, K.Rosenberg, K.Oellinger, "Regulation of apoptosis-associated lysosomal permeabilization", Springer, 2010 .
[12] N.W.Warneburg, M.E.Giucciardi, S.F.Bronk, G.J.Gores, "Tumor necrosis factor alpha associated lysosomal permeabilization is cathepsin B dependent",Am. J. Physiol-Gastroint Liver Physiol 283: G947 – G956, 2007.
[13] AE.Feldstein, NW. Werneburg, A.Canbay, "Free fatty acids promote hepatic lipotoxidity by stimulating TNF-alpha expression via a lysosomal pathway", Hepatology 40: 185 – 194, 2004.
[14] M.E. Giucciardi, S.F.Bronk, N.W.Werneburg, GJ.Gores, " cFLIBL prevents TRAIL-induced apoptosis of hepatocellular carcinoma cells by inhibiting the lysosomal pathway of apoptosis", Am. J. Physiol-Gastroint Liver Physiol 292: G1337 – G1346, 2007.
[15] E. Zhang, M.F. Kircher, M. Koch, L. Eliasson, S.N. Goldberg, E. Renström, „Dynamic Magnetic Fields Remote-Control Apoptosis via Nanoparticle Rotation", ACS nano, 8, 4, 3192-3201, 2014.

Martin Koch is a Dr.-Ing. and has worked for many years in industry and as a teacher at Universities. At present he is retired but still affiliated to some firms and to a couple of universities as independent researcher.

Joachim Wiest finished a doctorate on dissolved oxygen sensors for lab-on-chip systems at *Technische Universität München* in 2008. Since 2007 he is founder and chief executive officer of cellasys GmbH. In 2009 he took a University teaching position at his Alma Mater. Main fields of activity are system engineering, electrochemistry and biosensors.